

The role of interstitial oxygen on the structural and electrical properties of ZnO film grown by the pulsed laser deposition technique

E. CHAN Y DÍAZ^{a,c}, M. ACOSTA^b, R. CASTRO-RODRÍGUEZ^c, A. IRIBARREN^{c,d*}

^a*Departamento de Ingeniería Mecánica, Instituto Tecnológico de Mérida, Av. Tecnológico km. 4.5 s/n, 97118, Mérida, Yucatán, México*

^b*Materials Science Laboratory, Faculty of Engineering, University of Yucatan, CP 97130 Mérida, Yuc., México*

^c*Department of Applied Physics, CINVESTAV-IPN, Unidad Mérida, Km. 6 Antigua carretera a Progreso, Apdo. Postal 73, Cordemex, 97310, Mérida, Yuc., México*

^d*Instituto de Ciencia y Tecnología de Materiales (IMRE), Universidad de La Habana, Zapata y G, Vedado, La Habana 10400, Cuba*

ZnO thin films were deposited by the pulsed laser deposition technique under relatively low partial oxygen pressures between the minimum given under base vacuum and 5.33 Pa on glass substrates. The effects of the partial O pressure (p_{O}) within the chamber during the deposition on the structural and electrical properties were investigated. It was found preferential growth on the c axis. The (002) peak position moves from left to right of the ZnO powder pattern (002) peak. It is associated to the O vacancy passivation and the interstitial O formation as p_{O} increases which induces the c lattice parameter diminishes. The grain size asymptotically increases up to a value $D \approx 26$ nm as p_{O} increases. The ZnO film resistivity decreases with p_{O} , which is opposite to that expected. This controversial behavior was explained from the compensation of oxygen vacancy passivation and the predominance of interstitial configurations of oxygen plus interstitial Zn over p-type defects as antisite Zn atoms and Zn vacancies during the nucleation in the films. Such the assumption agrees and is validated by the diminishing of the c lattice parameter as a function of the p_{O} increasing.

(Received May 10, 2016; accepted August 9, 2017)

Keywords: ZnO, Laser deposition, Electrical resistivity, Defects, Interstitials

1. Introduction

ZnO is a II–VI semiconductor with a direct and wide band gap that ranges between 3.2 and 3.37 eV at room temperature [1-3]. It is a promising material given that it could be applied to many fields such as transparent conductive contacts, solar cells, laser diodes among other applications [4-7]. Undoped ZnO thin films typically exhibit n-type conductivity and are transparent to the visible light, with electron concentrations as high as 10^{21} cm⁻³ [8] mainly due to oxygen vacancies, although interstitial Zn is also present. The study of the ZnO defects remains in focus of researchers and not a few works have been directed to the elucidation of its electronic characteristics [9-16].

The pulsed laser deposition technique (PLD) has been used for obtaining ZnO films [17]. However, the fact it is a high-energy technique leads to think that the obtained film material can be highly defective, mainly due to be sub-stoichiometric in oxygen [18]. In order to mitigate the O defectivity several research groups have been using reactive atmospheres of oxygen in the growth chamber. With this proceeding changes in the oxygen vacancy concentration must be expected, which will induce changes in the material properties.

These studies have shown ZnO film conductivity dependence on the O pressure in the reaction chamber of high energy growth techniques as pulsed laser deposition [19-21]. Frequently, the conductivity of the ZnO films increases as the partial O pressure during the growth increases.

Authors have related this conductivity increase to improvement of stoichiometry by passivation of O vacancies and O absorption due to the increase of the partial O pressure [22,23], the reduction in grain boundaries [20], and so on. However, other authors have reported that the conductivity and carrier concentration diminish [24,25] as the O pressure increases.

In this work the behavior of the conductivity as a function of the partial O pressure in the PLD reaction chamber was related to the variation of ZnO lattice and took into account the defect formation energies. From our analysis we associated the carrier concentration increase with the O pressure to the predominance of donor defects as interstitial zinc and oxygen whose presence into the ZnO lattice affects these parameters.

2. Experimental section

ZnO thin films were deposited on corning glass 2947 substrates using a Nd:YAG laser at a repetition rate of 5Hz, operating in the Q-switch mode with energy density at the target ~ 2 J/cm² and 5000 laser shots. The target was a 10 mm diameter pressed and sintered solid disk made up of ZnO nanoparticles (99.99% Aldrich). Films were deposited at 6.7×10^{-4} Pa base vacuum and substrate temperature $T_s = 573$ K in a partial oxygen pressure, p_{O_2} , which ranged between about 1.3×10^{-4} Pa corresponding to the residual partial oxygen pressure in the chamber ($p_{O_2} \approx 0$) and 5.33 Pa. The structural properties were determined by measurements in the grazing incidence geometry with an inclination of 1.0° in the x-ray diffraction beam (XRD) by using CuK α monochromatic wavelength ($\lambda = 1.5405$ Å). Acquisition conditions were a beam of 40 kV with 35 mA and with an aperture diaphragm of 0.2 mm, using a D5000 Siemens X-ray diffractometer. The thickness of the films was measured by a surface profilometer Dektak-8 Veeco. Resistivity, electron concentration and mobility values were obtained with an Ecopia HMS-5000 Van der Pauw Measurement System at room temperature.

3. Results and discussion

3.1 XRD results and analysis

Fig. 1 shows the normalized diffractograms of the ZnO films for different partial O pressures. A comparison with the pattern [26] shows single-phase hexagonal with only ZnO wurtzite structure and preferential orientation in the plane (002). Low intensity (101), (102) and (103) plane peaks are also evidenced in the XRD diffractograms. Lorentzian fitting was applied to diffraction peaks. Fig. 2a and 2b show the resultant (002) peak positions (2θ) and its full width at half maximum (FWHM) as functions of the partial O pressure. A line at the (002) peak position of the ZnO pattern is also drawn in Fig. 2a. For low O pressure the peaks are shifted toward angles below that of the pattern, which correspond to extended or tensed lattice due to the O vacancy concentration is relatively high and the Zn atom neighbors move toward the void left by the O atom and the interatomic bonds increase. The behavior indicates that the lattice tends to the pattern angular values as p_{O_2} increases. This is presumably due to O atmosphere contributes to passivate the O vacancies and its effect over the lattice reduces. For higher O pressure the (002) peaks shift to angles higher than that of the pattern, which is sign of a shrunk or compressed lattice.

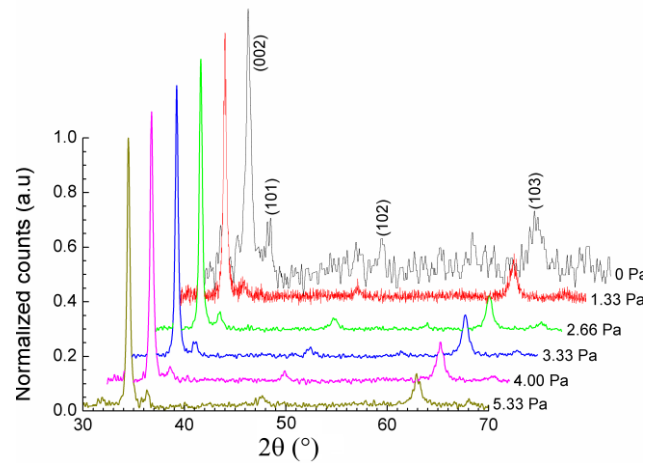


Fig. 1. Diffractograms of ZnO films as a function of the O partial pressure

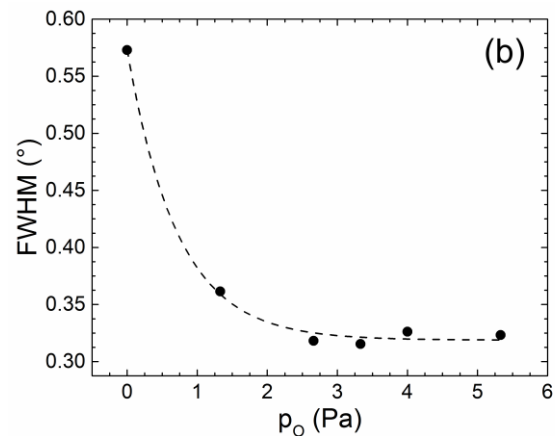
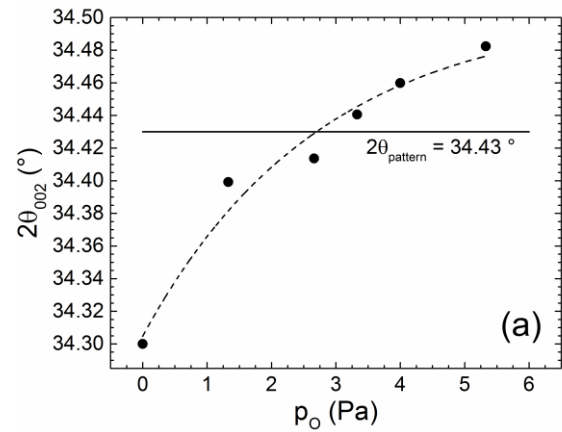


Fig. 2. 2θ angle (a) and FWHM (b) of the (002) peak as functions of the O partial pressure, p_{O_2} . Dashed lines only represent mathematical fittings

The O pressure dependence of FWHM shows a sharp diminishing for low p_O up to asymptotically reach a value $\text{FWHM} \approx 0.321^\circ$ ($\pm 0.002^\circ$), which indicates that the disorder does not significantly increase. Fig. 3 shows the crystallite size obtained from the Scherrer formula [27]:

$$D = \frac{0.9 \lambda}{\text{FWHM} \cos \theta} \quad (1)$$

where $\lambda = 0.15405$ nm is the x-ray wavelength. The calculated crystallite size increases from $D \approx 16$ nm for $p_O \approx 0$ Pa, up to an asymptotic value $D \approx 26.1$ nm (± 0.2 nm).

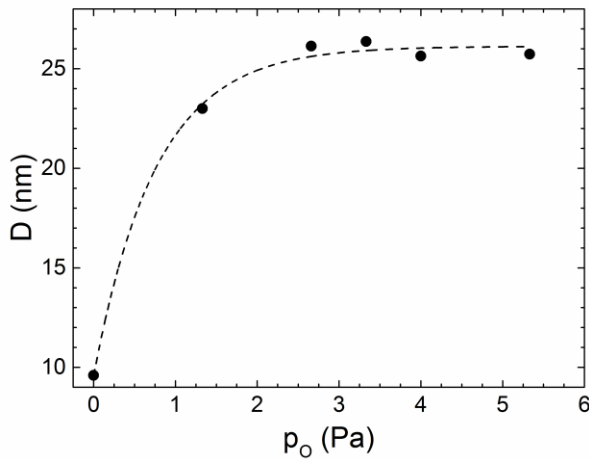


Fig. 3. Variation of the effective grain size as a function of the O partial pressure, p_O . The dashed line is an asymptotic fitting

For calculating the lattice parameters we used the expression for hexagonal crystals [27]:

$$\sin^2 \theta = \frac{\lambda^2}{4} \left[\frac{4}{3} \times \frac{(h^2 + hk + k^2)}{a^2} + \frac{l^2}{c^2} \right] \quad (2)$$

where h , k , and l are de Miller indices and a and c are the lattice parameters. The c parameter was estimated with the expression (2) using the (002) peak angle. It was found that c parameter in $p_O \approx 0$ conditions is longer due to the inward relaxation of the Zn surrounding the O vacancies. As p_O increases c diminishes and tends to the pattern c parameter as displayed in Fig. 4, which is due to the O vacancy passivation. For the highest O pressures the lattice becomes compressed and reaches values below that of the pattern for highest p_O . The lattice distortion over the c axis was calculated from $\Delta c/c_0$ where $\Delta c = c - c_0$, and $c_0 = 0.5205$ nm is the pattern c parameter [26]. It was found that the c distortion diminishes as p_O increases. a and b parameters did not displayed a clear tendency and it was considered practically invariable with a mean values $a = b \approx 0.325$ nm (± 0.002 nm) and a lattice strain $\Delta a/a_0 \approx -0.12\%$, where $a_0 = 0.3248$ nm is the pattern a parameter [26].

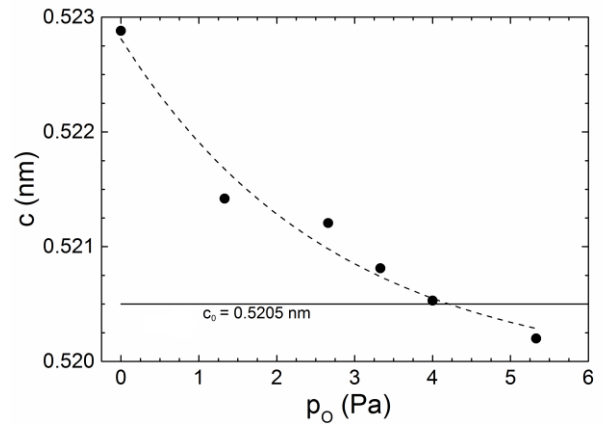


Fig. 4. c -parameter behavior as a function of p_O . The dashed line is a mathematical exponential fit

Results indicate that the lattice is tensed for low p_O , and compressed for high p_O over the c axis, but practically remains invariant over a and b axis. FWHM, D and c -parameter distortion behaviors indicate that the material structure improves its organization as the O pressure increases, although for highest p_O the lattice structure again worsens. Nevertheless an asymptotic fitting give a tendency to $c_{\min} = 0.5199$ nm (± 0.0007 nm), which corresponds to a c -axis lattice distortion as low as $\Delta c/c_0 \approx -0.1\%$. We associate the reduction of c values to saturation of the ionized and neutral defect passivation and formation. Table 1 summarizes the main parameters obtained from the structural analysis, where the lattice distortion over the c axis was included.

Table 1. Parameters obtained from the structural analysis

p_O (Pa)	2θ ($^\circ$)	FWHM ($^\circ$)	$\Delta c/c_0$ (%)	D (nm)
0	34.31	0.522	0.00634	15.9
1.33	34.40	0.362	0.00177	23.0
2.66	34.41	0.318	0.00136	26.1
3.33	34.44	0.315	5.99×10^{-4}	26.4
4.00	34.46	0.326	5.78×10^{-5}	25.6
5.33	34.48	0.323	-5.76×10^{-4}	25.7

3.2. Electrical results and analysis

The resistivity of the films present presents a practically linear behaviour as shown in Fig. 5. It is directly related to the electron concentration and mobility, which are plotted in Fig. 6. However, an inverse behaviour of the resistivity must be expected, because the increase of p_O in the reaction chamber induces that O atoms passivate the O vacancy natively present in the material. Thus, as the electron concentration must diminish and according to the expression for the resistivity, ρ :

$$\rho = \frac{1}{en\mu} \quad (3)$$

where e is the electron charge, n is the electron concentration and μ the electron mobility, the resistivity

must consequently increase. From the experimental resistivity and the calculated electron concentration, the electron mobilities were calculated from Eq. 3. As observed in Fig. 6 the electron concentration increases and tends to a constant value, and the mobility diminishes as increases p_O . Table 2 shows the results of electrical measurements.

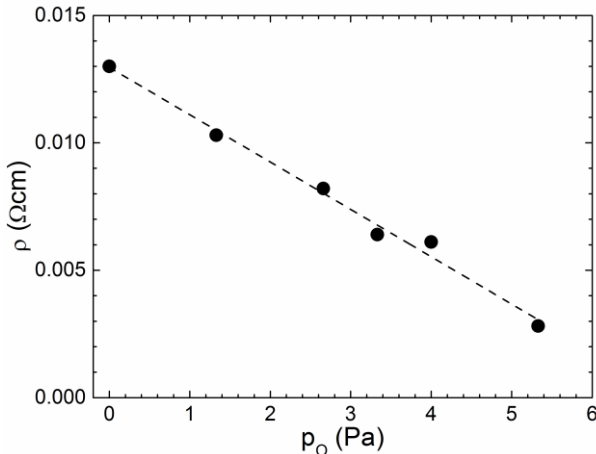


Fig. 5. Resistivity of the ZnO films as a function of the O partial pressure, p_O . The dashed line is a mathematical linear fit

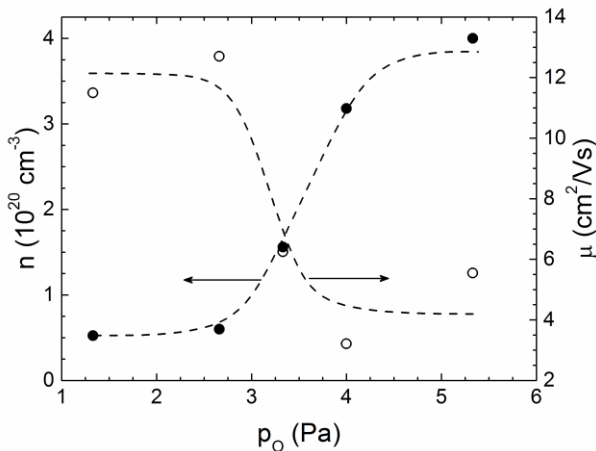


Fig. 6. Electron concentration (•) and mobility (–) as functions of the O partial pressure, p_O . The dashed curves only represent the tendency

Table 2. Results obtained from the electrical measurements

p_O (Pa)	ρ (Ωcm)	n (cm^{-3})	μ ($\text{cm}^2\text{V}^{-1}\text{s}^{-1}$)
0	0.013	-	-
1.33	0.0103	5.25×10^{19}	14.4
2.66	0.00821	5.99×10^{19}	15.2
3.33	0.0064	1.56×10^{20}	5.7
4.00	0.00611	3.18×10^{20}	3.4
5.33	0.00281	4×10^{20}	5.6

The diminishing of the c parameter and the lattice strain agree with the O vacancy passivation. However, we consider that it is only a predominant structural effect and

other defect effects are also present in such a way that, although they do not initially influence on the lattice, they do influence predominantly on material electronic characteristics.

The defect in native ZnO can be grouped as donor and acceptor. The donor defects are di-, monoionized and neutral interstitial Zn, $\text{Zn}_i^{\bullet\bullet}$, Zn_i^\bullet , Zn_i^0 , di-, monoionized and neutral O vacancies, $\text{V}_O^{\bullet\bullet}$, V_O^\bullet , V_O^0 , and antisites Zn, Zn_O . The acceptor defects are di- and monoionized and neutral Zn vacancies, $\text{V}_{\text{Zn}}^{\bullet\bullet}$, $\text{V}_{\text{Zn}}^\bullet$, V_{Zn}^0 , and antisite O, O_{Zn} [28-30]. O_i can present several configurations into the lattice and it has been suggested that O_i charges whether positively and acts as donor defect or negatively and acts as acceptor defect [30-32]. In our case, as the electron concentration increases and it is a fact that a partial O vacancies passivation takes place, which, conversely, induces reduction of electron concentration, we have to assume that donor defects are predominantly acting.

For O-rich condition the formation energies of Zn vacancies is the lowest, although the formation energy of interstitial O and antisites O also diminish for high Fermi levels [30,31], which favor the concentration of these defects. In the same way, the formation energy of interstitial O has been found diminishing in O-rich conditions. O_i could have relatively high concentration [33] and even be the dominant defect [31]. Other defects as Zn_i and Zn_O can be favored in growth processes under non-equilibrium conditions as it is our case [30]. Additionally extended donor Zn_i states likely formed from ionized, complex and localized Zn_i has been also suggested [29], which increases the density of localized states of this defect. All these defects induce n-type conductivity, and, according to the conductivity values found in our work, are dominant over the Zn vacancies, and any other p-type defects, although V_{Zn} is supposedly the most favored defect due to its low formation energy [30,31]. From these considerations we can infer that the reduction of c parameter as O partial pressures increases is due O vacancy passivation. However, for higher O pressures the V_O concentration is relatively very low and the influence of other defects starts getting more significant. However, the distortion produced by these defects is smaller than that of V_O , which explains the lattice distortion reaches a value modularly six times smaller than that of native ZnO with $p_O \approx 0$ Pa.

O atoms have size smaller than a half than that of Zn. Then, both O atoms in Zn sites and Zn vacancies induce the interatomic distance increases and, in fact, lattice constant expands due inward relaxation. However, the structural behavior is of outward relaxation, which agrees with interstitial O that mainly places over the c axis, but stimulating an additional O-O bond as was previously proposed [30,31]. Therefore, we can consider that O_i predominates over O_{Zn} and V_{Zn} . On the other hand, as the lattice enhances its organization, the diminishing of electron mobility can be associated to be limited by ionized defect or inter-electron scattering.

We can venture that this phenomenon can also take place in high-energy growth techniques, as rf-sputtering, which favor the presence of ionized O species that reactively arrive in the substrate, although obviously with some differences in the growth conditions.

4. Conclusions

We found that for ZnO films grown by the PLD technique and changing the O partial pressure in the growth chamber the structure improves, the resistivity decreases and the electron concentration increases in the films. According to this oxygenized process the electrical behavior should be different. We made an analysis about the factors that intervene in the process and are present in the material film. Thus, we concluded that in the ZnO film deposition under an O atmosphere, a passivation process of the O vacancies took place, but simultaneously several defects with donor behavior as interstitial Zn and O dominate over those p-type defects, giving a compensated n-type material.

Acknowledgments

Authors thank Oswaldo Gómez, Mario Herrera, Wilian Cauich, Daniel Aguilar, and E. A. Martín Tovar for technical assistance and to Lourdes Pinelo for secretary assistance. This work has been supported by the Project No. CB/2012/178748 CONACYT/México. One of the authors (A. Iribarren) thanks to CONACYT/México under the program No. 260967 for sabbatical stances for Mexican and foreign researchers living abroad for supporting this research and to the Project PNCB-51-UH-15, Cuba.

References

- [1] P. R. Willmott, J. R. Huber, *Rev. Mod. Phys.* **72**, 315 (2000).
- [2] H. S. Kim, H. S. Kwok, *Appl. Phys. Lett.* **61**, 2234 (1992).
- [3] A. Iribarren, P. Fernández, J. Piqueras, *Superlattices Microst.* **43**, 600 (2008).
- [4] J. Xu, K. Fan, W. Shi, K. Li, T. Peng, *Sol. Energy* **101**, 150 (2014).
- [5] M. Raja, N. Muthukumarasamy, D. Velauthapillai, R. Balasundaraprabhu, S. Agilan, T. S. Senthil, *Sol. Energy* **106**, 129 (2014).
- [6] M. Seghatoleslami and R. Forutani, *J. Adv. Agric. Technol.* **2**, 34 (2015).
- [7] C. Gomez-Solís, J. C. Ballesteros, L. M. Torres-Martínez, I. Juárez-Ramírez, L. A. Díaz Torres, M. E. Zarazua-Morina, S. W. Lee, *J. Photoch. Photobio A: Chem.* **298**, 49 (2014).
- [8] T. A. Krajewski, Kr. Dybko, Gr. Luka, El. Guziewicz, P. Nowakowski, B. S. Witkowski, R. Jakiela, L. Wachnicki, A. Kaminska, A. Suchocki, M. Godlewski, *Acta Mater.* **65**, 69 (2014) and references there in.
- [9] J. Wang, Z. Wang, B. Huang, Y. Ma, Y. Liu, X. Qin, X. Zhang, Y. Dai, *ACS Appl. Mater. Inter.* **4**, 4024 (2012).
- [10] X. Li, Y. Wang, W. Liu, G. Jiang, Ch. Zhu, *Mater. Lett.* **85**, 25 (2012).
- [11] H. Liu, F. Zeng, Y. Lin, G. Wang, F. Pan, *Appl. Phys. Lett.* **102**, 181908 (2013).
- [12] J. Santana, J. T. Krogel, J. Kim, P. R. C. Kent, F. A. Reboledo, *J. Chem. Phys.* **142**, 164705 (2015).
- [13] Ü. Özgür, D. Hofstetter, and H. Morkoç, *P IEEE* **8**, 1255 (2010).
- [14] E. G. Goh, X. Xu, P. G. McCormick, *Scripta Mater.* **78–79**, 49 (2014).
- [15] J. Timoshenko, A. Anspoks, A. Kalinko, A. Kuzmin, *Acta Mater.* **79**, 194 (2014).
- [16] T. A. Krajewski, K. Dybko, G. Luka, E. Guziewicz, P. Nowakowski, B. S. Witkowski, R. Jakiela, L. Wachnicki, A. Kaminska, A. Suchocki, M. Godlewski, *Acta Mater.* **65**, 69 (2014).
- [17] R. Kumar, G. Kumar, A. Umar, *J. Nanosci. Nanotechnol.* **14**, 1911 (2014).
- [18] S. Choopun, R. D. Vispute, W. Noch, A. Balsamo, R. P. Sharma, T. Venkatesan, A. Iliadis, D. C. Look, *Appl. Phys. Lett.* **75**, 3947 ((1999)).
- [19] E. Fazio, S. Patanè, S. Scibilia, A. M. Mezzasalma, G. Mondio, F. Neri, S. Trusso, *Curr. Appl. Phys.* **13**, 710 (2013).
- [20] L. P. Ling, H. M. Khen, T. K. Chu, D. N. Kumari, Y. S. Shan, O. B. Hoong, T. T. Yong, *IJNeAM* **8**, 7 (2015).
- [21] P. Gondoni, M. Ghidelli, F. Di Fonzo, V. Russo, P. Bruno, J. Martí-Rujas, C. E. Bottani, A. Li Bassi, C. S. Casari, *Thin Solid Films* **520**, 4707 (2012).
- [22] P. S. Shewale, S. H. Lee, N. K. Lee, Y. S. Yu, *Mater. Res. Express* **2**, 046401 (2015).
- [23] Ch.-F. Yu, Ch.-W. Sung, S.-H. Chen, Sh.-J. Sun, *Appl Surf. Sci.* **256**, 792 (2009).
- [24] Ö. Hadis Morkoç, *Zinc Oxide: Fundamentals, Materials and Device Technology*, Wiley-VCH Verlag GmbH & Co. KGaA, Weinheim, 2009.
- [25] L. P. Ling, H M Khen, T. K. Chu, D. N. Kumari, Y. S. Shan, O. B. Hoong, T. T. Yong, *IJNeAM* **8**, 7 (2015).
- [26] JCPDS-International Centre for Diffraction Data. 2003, PCPDFWIN v. 2.4. Chart No. 89-0510.
- [27] B. D. Cullity, *Elements of x-ray diffraction*, Addison-Wesley Publishing Company, Inc. Massachusetts, USA, 1956.
- [28] L. Schmidt-Mende, J. L. MacManus-Driscoll, *Mater. Today* **10**, 40 (2007).
- [29] P. Erhart, A. Klein, K. Albe, *Phys. Rev. B* **72**, 085213 (2005).
- [30] A. Janotti, Ch. G. Van de Walle, *Rep. Prog. Phys.* **72**, 126501 (2009).
- [31] H. Zeng, G. Duan, Y. Li, Sh. Yang, X. Xu, W. Cai, *Adv. Funct. Mater.* **20**, 561 (2010).
- [32] A. Sahai, N. Goswami, *Ceram. Int.* **140**, 14569 (2014).
- [33] S. K. Pandey, S. K. Pandey, U. P. Deshpande, V. Awasthi, A. Kumar, M. Gupta, and S. Mukherjee, *Semicond. Sci. Technol.* **28**, 085014 (2013).

*Corresponding author: a_iribarren@yahoo.com, augusto@imre.uh.cu